Fall 11-24-1961

An Investigation of Indeterminate Structures Stressed Beyond the Proportional Limit

Jack B. Joyce

AN INVESTIGATION OF INDETERMINATE STRUCTURES STRESSED BEYOND THE PROPORTIONAL LIMIT

By

Jack B. Joyce

A Thesis

Submitted in Partial Fulfillment of the Requirements

for the Degree of Master of Science in Civil Engineering

The University of New Mexico

1961

This thesis, directed and approved by the candidate's committee, has been accepted by the Graduate Committee of the University of New Mexico in partial fulfillment of the requirements for the degree of

MASTER OF SCIENCE

Stuart A. Northrop
Dean

November 29, 1961
Date

Thesis committee

Eugene Zwoyer
Chairman

M. M. Cottrell

A. H. Clough

PREFACE

This thesis is offered as an addition to the work presently being done in the field of ultimate load design. It was prepared as the independent work required for the Master of Science degree in civil engineering. While practical conditions limited the extent of the study, it is hoped that further efforts in this field will be aided to some extent.

All of the work described was concerned with behavior of aluminum alloys stressed beyond the elastic limit. Of particular interest was the prediction of moment distribution in indeterminate frames since conventional elastic method cannot be used after any portion of the structure experiences stresses beyond the elastic limit. For this purpose an approximate method of reasonable simplicity and accuracy was used. The predicted values were compared with test results run on a frame of the same dimensions and material.

The writer would like to acknowledge the far reaching assistance and cooperation of Dr. Eugene Zwoyer in making this paper possible.

CONTENTS

SYMBOLS AND NOTATIONS

b	width of section
B	modulus of plasticity
c	distance from neutral axis to extreme fiber
E	modulus of elasticity
e	total strain at point denoted by subscript
f	stress
h	depth of section
I	moment of inertia of section
K	stress intercept of assumed stress-strain curve
L	span
m	$\frac{M}{zk}$
M	bending moment
n	$\frac{Eh\rho}{2K}$
P	$\int \rho dM$
q	proportional limit of assumed curve
Q	$\int \rho M d M$
r	modular ratio -- $\frac{B}{E}$
R	radius of curvature

S	shape factor
W	load
x	distance along member
y	distance from neutral axis
z	section modulus
Δ	total deflection
ϕ	$\frac{Eh}{KM} \cdot P$
δ	$\frac{2}{3} \cdot \frac{Eh}{KM^2} \cdot Q$
ϵ	unit strain
ρ	curvature

SUBSCRIPTS

c	compression or pertaining to distance to extreme fiber
t	tension
ult.	ultimate

INTRODUCTION

Methods follow materials. This is an unwritten rule that has been true in creative work throughout the years. Each time a new material is offered to the imaginative mind unique methods are derived to exploit its different features. The process is continuous with refinements coming one after another as a deeper study of the material is made.

In the structural field the methods of designing have been geared to the development of materials. The advent of structural steel and reinforced concrete was the most outstanding example of materials suggesting methods in the modern age. With these two materials the designer was offered the possibility of lightweight construction in large structures. But to make this potential a reality construction methods had to be revised. To have continued in the previous vein would have been to ignore all of the economic and aesthetic possibilities implied in the new materials. Out of this rejuvenation came systems for predicting the behavior of continuous beams, two way slabs, beam-columns, and the endless other ways of using modern construction materials.

In a more current appraisal we see steel and concrete being updated still further. Pre-stressed concrete is a common sight in present day construction work and, to a lesser extent, the educated eye sees rigid frames designed to ultimate load criteria. Here again are cases where materials are studied and found to possess characteristics that are adaptable to advanced methods. The key to all such improvements is the realization and the utilization of material properties.

While it can be said that "nothing is new under the sun", in a practical sense "new" things are presented to us every day. In the materials field the structures engineer is currently being offered products that would not be called new in concept but are certainly different in application. In one area we see the lightweight alloys and alloy steels. These two metal groups are lumped together because of their purpose in reducing total structural weight and in their behavior under load.

A compromise including all of the features mentioned is the aluminum alloy 6061-T6. The T6 temper refers to a heat treatment and artificial aging leading to a reasonably high yield strength. A yield and ultimate tensile strength of 35 and 38 ksi respectively was suggested in the ASCE Proceedings[1]. Review of the Mil-HDBK-5[2] shows these values to be the lowest minimum guaranteed values for extruded shapes of 6061-T6. The other recommendations such as corrosion resistance, weldability, etc., show the material to be desirable from a standpoint of versatility.

The next phase in examining the material is a detailed investigation of its behavior under load. Here we see a sharp variation from that of structural steel, which has been a standard in past work. Figure 1 shows a general comparison between the stress-strain curves of mild steel and aluminum alloys.

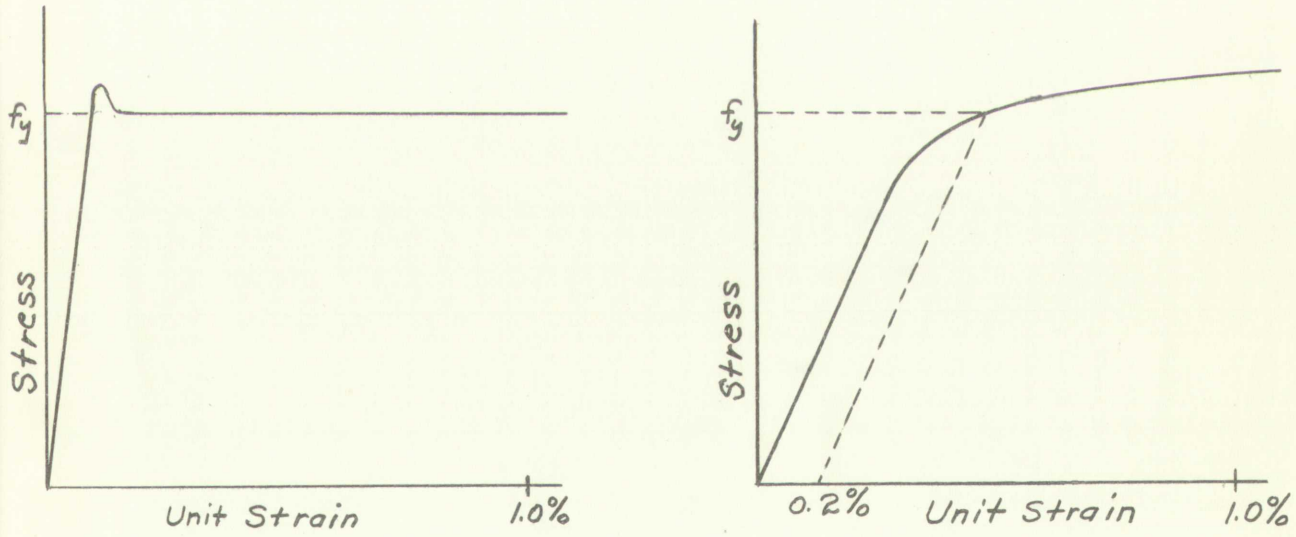

Mild Steel Aluminum

Figure 1

The elastic portions of both materials are followed by regions of rapidly increasing strain resulting from only slight increases in stress. In mild steel the assumed curve, in the range shown, depicts strain increasing from the initial yield strain to several times that value without an increase in stress. Tests demonstrate this to be a reasonable approximation. The aluminum alloys do not follow this pattern. From the proportional limit to some excessive strain point approaching rupture, the relation between stress and strain is constantly changing. The slope of the stress-strain curve describing this relationship decreases continuously from the proportional limit to failure.

This difference in behavior of mild steel and aluminum alloy as described in Figure 1 outlines the complete purpose of this paper. Up to the present time most structural design has been based on purely elastic considerations or a combination of elastic and plastic strains as they occur in mild steel. Beyond the proportional limit the assumption is made that strain will increase without added stress. This latter recognition forms the basis for the Plastic Design[3] or Limit Load method now being used in mild steel design and analysis.

Exception can easily be taken with the suggestion that plastic strains of the type displayed by aluminum alloys have not been recognized and utilized by many analysts and designers. Timoshenko[4] presented a method of determining the exact resisting moment in a material where the dissimilar but known tension and compression stress-strain curves are available.

Panlilio[5] suggested that the increase of strain with load in continuous light alloy beams was a definite advantage since all sections provided positive moment resistance until collapse. He felt that this bonus performance out-weighed the difficulty in realistically utilizing such behavior. The point was well made but no method was given for determining, for a general case, the safety factor against failure that one could expect.

Cozzone[6] in 1943 published a very comprehensive and practical paper on designing for ultimate load in light alloys. His method was primarily concerned with insuring that stress levels at ultimate load did not exceed a desired amount. The increased load carrying ability of the material was recognized and accounted for by using an approximate stress-strain relationship. Figure 2 shows the form of the assumed curve versus the actual. Curve odbc gives the true stress-strain reaction of a material to load, while oabc is the assumed shape. The fictitious stress f_o is chosen in conjunction with a desired f_m to give a moment about the stress axis equal to that of the true curve.

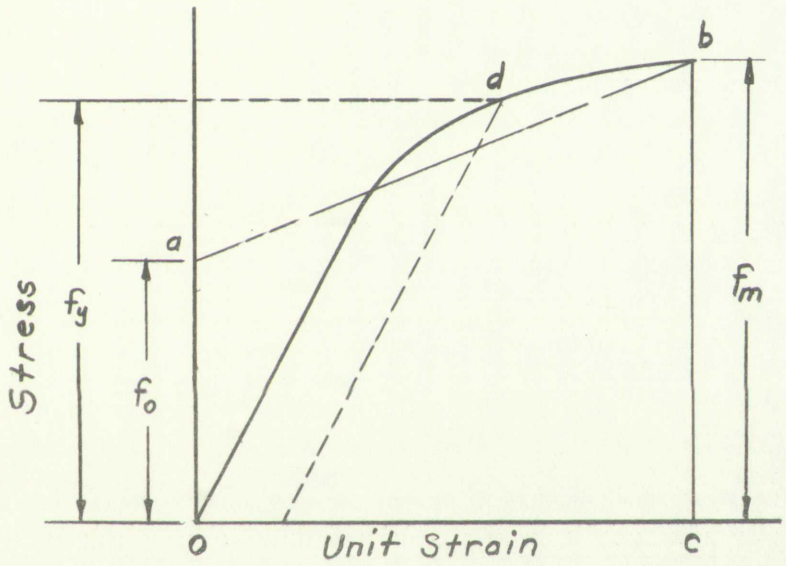

Figure 2

It can be seen that each change in f_m would mean a change in f_o. This presents no undue hardship if only stress information at some arbitrary ultimate strain is desired. For a continuous review of structural performance from the time the proportional limit is first reached in a structure until ultimate load is reached several values of f_o would be required.

Each of these contributions, along with numerous others, has improved the insight into ultimate design in high strength-to-weight alloys. In each, however, conditions of loading at a point in question are assumed to be known. The area of broadest study has been concentrated on the relationship of stress and strain at a point without including the redistribution of resistance throughout the structure. If the assumed conditions at a point can be verified by continuity considerations for the entire structure, then the solution cannot be questioned. In most cases of an indeterminate structure, stressed beyond the proportional limit, a trial and error appraisal of assumed loading distributions becomes prohibitively lengthy.

One possible approach for relatively simple cases, indeterminate to the first degree, can be established by using two boundary conditions. First, the desired "ultimate" moment must be established for the particular alloy, and the size and shape of the section under investigation. Secondly, an elastic moment distribution must be established noting the point which is most highly stressed. With these two pieces of information and the realization that the most highly stressed elastic point will also reach the ultimate permissible strain no later than any other point, a static solution can be achieved by simply introducing the ultimate moment as the actual moment at that point. An example is shown in Figure 3. The frame has pinned ends and is indeterminate to the first degree. Either M_b or M_c could cause the higher stress depending on the geometry and comparison of section moduli and moments of inertia of the members. Assuming the stress at B to be the larger, member AB could be removed as a free body with $M_{ult.}$ at B and the horizontal reaction at A determined. The frame is thus reduced to the determinate case. It should be noted that the use of the most highly stressed elastic point as the location of ultimate moment is only valid for structures whose members have roughly the same reserve strength (shape factor). Behavior of a structure using

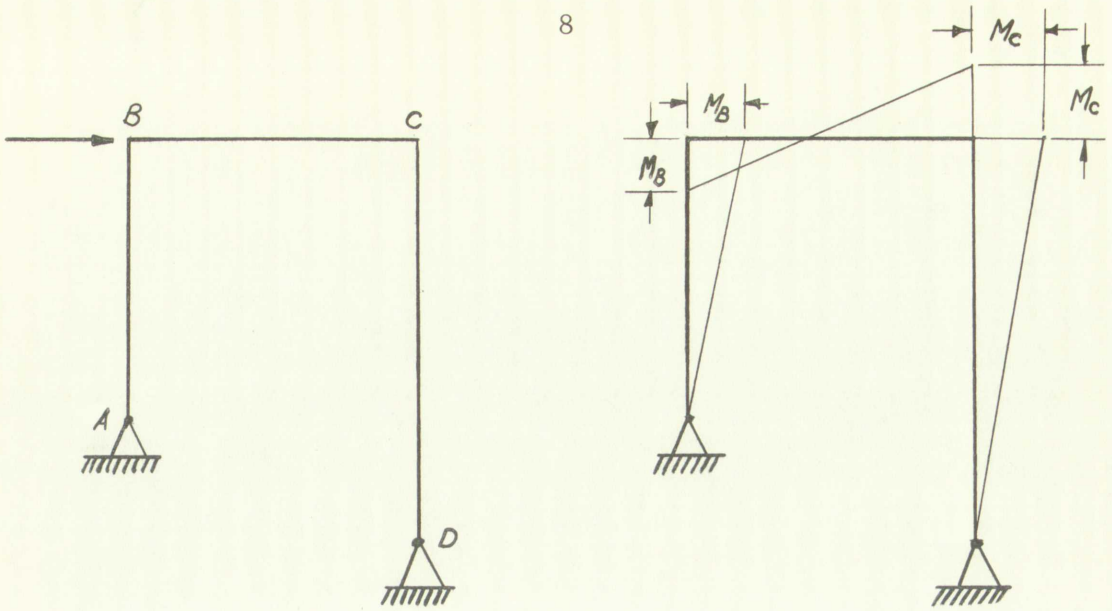

Figure 3

members with shape factors running from 1.2 to 2.0 could not be handled in so simple a manner.

The limitations of such a simplified method are numerous. Any general approach should be able to include all shape factors, degrees of indeterminance, and prediction of deflections as well as stresses at any loading up to the desired ultimate point.

The difficulty in determining such information is all caused by the variable relationship between stress and strain above the proportional limit. Another approach at solving the problem is a mathematical one. Most curves can be represented by some expression relating the variables. Indeed Young's Modulus is nothing more than such an expression. The problem in the alloys centers around the complexity of such expressions. Some of the most promising mathematical approaches were offered by Wang[7], Osgood[8], Beilschmidt[9] and Gill[10]. Each of these authors presented equations that related the variables, stress and strain. With the proper choice of constants and exponents such equations could display satisfactory agreement with stress-strain curves of a particular material. Their shortcoming again centered around the complexity of a system utilizing such equations.

Dwight[11], in his work for The Aluminum Development Association, reviewed proposed methods for dealing with alloys and detailed an approach based on use of a two slope or two moduli curve that approximates the elastic and plastic behavior of a material. The idea is not new but its application is, in defining the redistribution of moments beyond the elastic range. The remaining presentation in this paper is a review and extension of the work done by Dwight.

MOMENT CURVATURE RELATIONS

Bending strains in the plastic range cannot be determined by using all of the methods of conventional analysis but some relationships are still quite valid. When a cross section is subjected to a known moment its behavior, relative to a cross section a small incremental distance away, can be predicted. This is true in the elastic range if the modulus of elasticity is known and it is just as true in the plastic range if the stress-strain characteristics beyond the proportional limit are known. As an example, consider a rectangular cross section with a known moment applied. The tension and compression stress-strain curves are dissimilar but available. As in the elastic range, stress-strain curves derived from axial load tests are used to give tension and compression properties in bending. For the materials considered, this is a reasonable approximation. In Figure 4a the elastic distribution is given.

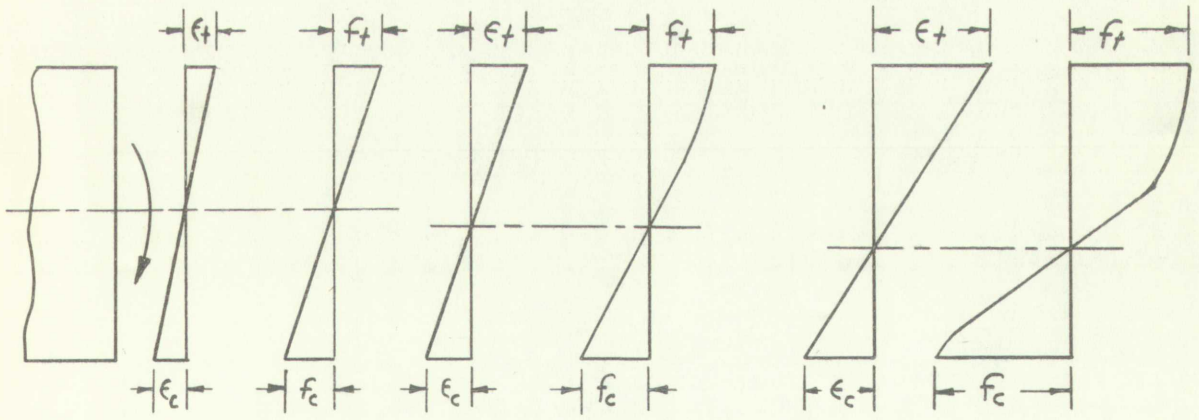

Figure 4

Figure 4b shows the tensile stresses and strains in the plastic region. The strain remains proportional to its distance from the neutral axis. This is a graphic presentation of the reasonable assumption that plane sections remain plane even beyond the proportional limit. Conditions of equilibrium require that the summation of tensile forces equal the summation of compressive forces and that the moment developed by these two equal the imposed moment. For this to be true in the case of a material with dissimilar tension and compression properties, the neutral axis must be displaced from the geometric center line. Finally, in Figure 4c, a critical strain is reached and the ultimate moment carrying capacity of the member is developed. As stated previously, with the applied moment known and the material properties available, a complete force and strain picture is drawn for the cross section. The curvature at a particular section can also be co-ordinated with moment, stress, and strain.

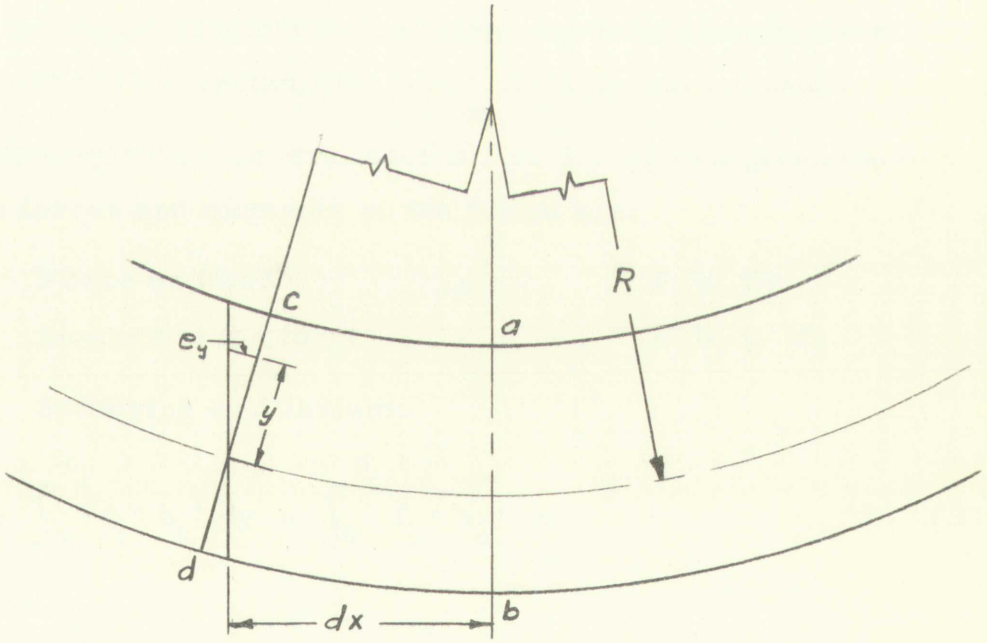

Figure 5

In Figure 5 we depict two sections of a loaded member with a radius of curvature R, and center line separation dx. Before loading, sections ab and cd are parallel. After loading the relationships are as seen in Figure 5 and from similar triangles:

$$\frac{R}{dx} = \frac{y}{e_y} \qquad \text{and} \qquad \epsilon_y = \frac{e_y}{dx}$$

$$\therefore \quad \epsilon_y = \frac{y}{R} \tag{1}$$

$$\epsilon_t = \frac{c_t}{R} \tag{2}$$

$$\epsilon_c = \frac{c_c}{R}$$

It can be seen that all of the foregoing expressions are presented in a general sense with the single assumption that plane sections remain plane. The use of a section other than rectangular would yield the same result.

Continuing with a general section, subjected to a given moment, we see that the forces and moments on the fibers are:

Force on fiber = $f \cdot b \cdot dy$

Moment of the force = $f \cdot b \cdot y \cdot dy$

Satisfying equilibrium:

$$F = \int_o^{c_t} f_t \cdot b_t \cdot dy = \int_o^{c_c} f_c \cdot b_c \cdot dy \tag{3}$$

$$M = \int_o^{c_t} f_t \cdot b_t \cdot y_t \cdot dy + \int_o^{c_c} f_c \cdot b_c \cdot y_c \cdot dy \tag{4}$$

With equations (2), (3), and (4) and the stress-strain curves relating ϵy to fy, a moment curvature diagram can be drawn.

At this point it is worthwhile to note some special circumstances that considerably simplify the analytical task. In the general case for any unsymmetrical cross section with dissimilar tension-compression properties the neutral axis for bending could move away from the centroid after the proportional limit is exceeded. It could not only move once, but could continue to move until the ultimate condition was reached. The location must be known to establish the limits of equations (3) and (4). With the variation of both stress and cross sectional dimensions for each increment dy, the problem is rather involved. For practical purposes a single stress-strain diagram for both tension and compression could be used. The error involved when considering most structural materials is quite small and very often outweighed by other assumptions such as homogeneity of the material, members initially straight, and material properties are minimum guaranteed. Secondly, the problem of unsymmetricl cross sections can be relieved by noting that most structural shapes, used to resist bending moments, have an axis of symmetry perpendicular to the plane of bending. If both of these special cases apply, and it is reasonable to assume that they do in most cases, the location of the neutral axis will continue to pass through the centroid under all increments of load. The bending moment can be given as:

$$M = 2 \int_{o}^{\frac{h}{2}} f \cdot b \cdot y \cdot dy \qquad (5)$$

With these methods at hand we have the basis for determining the ultimate moment that a section can resist.

The moment-area relationships are quite often used in structural analysis for determination of angular rotations and deflections. The physical characteristic of the method is use of the $\frac{M}{EI}$ versus span diagram. As we have shown, moment continues to be a meaningful quantity but elastic modulus and moment of inertia lose their singular significance when strains beyond the proportional limit are in evidence. With the same goal in mind it is worthwhile to try and establish similar tools for determining rotation and deflection without use of methods valid only for elastic conditions.

In Figure 6 we see a portion of a member loaded in bending much the same as in Figure 5.

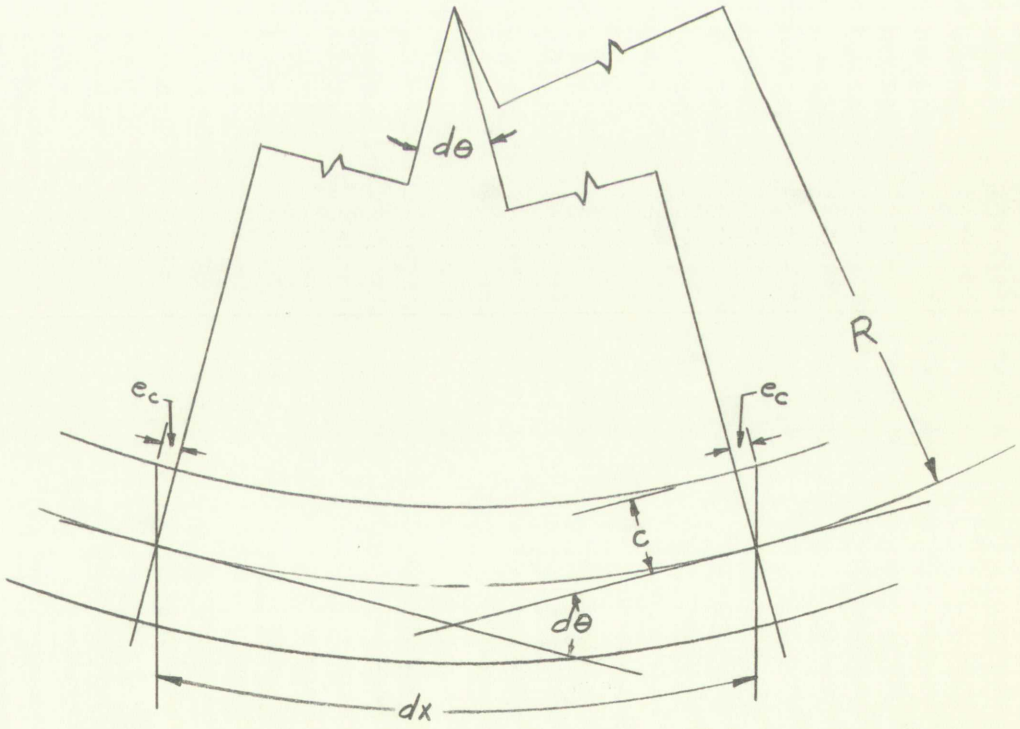

Figure 6

The following geometric observations can be made:

$$\frac{R}{c} = \frac{dx}{2e}$$

$$2e = d\theta \cdot c$$

$$\rho = \frac{1}{R} \quad \text{(by definition)}$$

$$\therefore \quad d\theta \cdot c = \rho c dx$$

Summing up the incremental variation we have:

$$\int_o^\theta d\theta = \int_o^x \rho dx \qquad (6)$$

$$\therefore \quad \theta = \text{Area under } \rho \text{ versus x diagram}$$

In this way we draw a parallel to the first moment area theorem. All of the relationships leading to equation (6) are equally true for both elastic and plastic conditions since strain rather than stress varies with change in geometry.

Summing up the information at hand for solution of rotations and deflections of determinate spans in either the elastic or plastic ranges we have:

1. Moment diagram for span
2. Extreme fiber stress from equations (4) or (5)
3. Extreme fiber strain from suitable stress-strain curve
4. Curvature of a section from equation (2)
5. Construction of a curvature versus span diagram
6. Determination of rotation between stations as the area of the curvature diagram between these same stations. This step can be accomplished by use of equation (6) or graphic means.

Another way of presenting these steps can be shown in the following manner. A span loaded only with end moments is used. Figure 7 shows the general case.

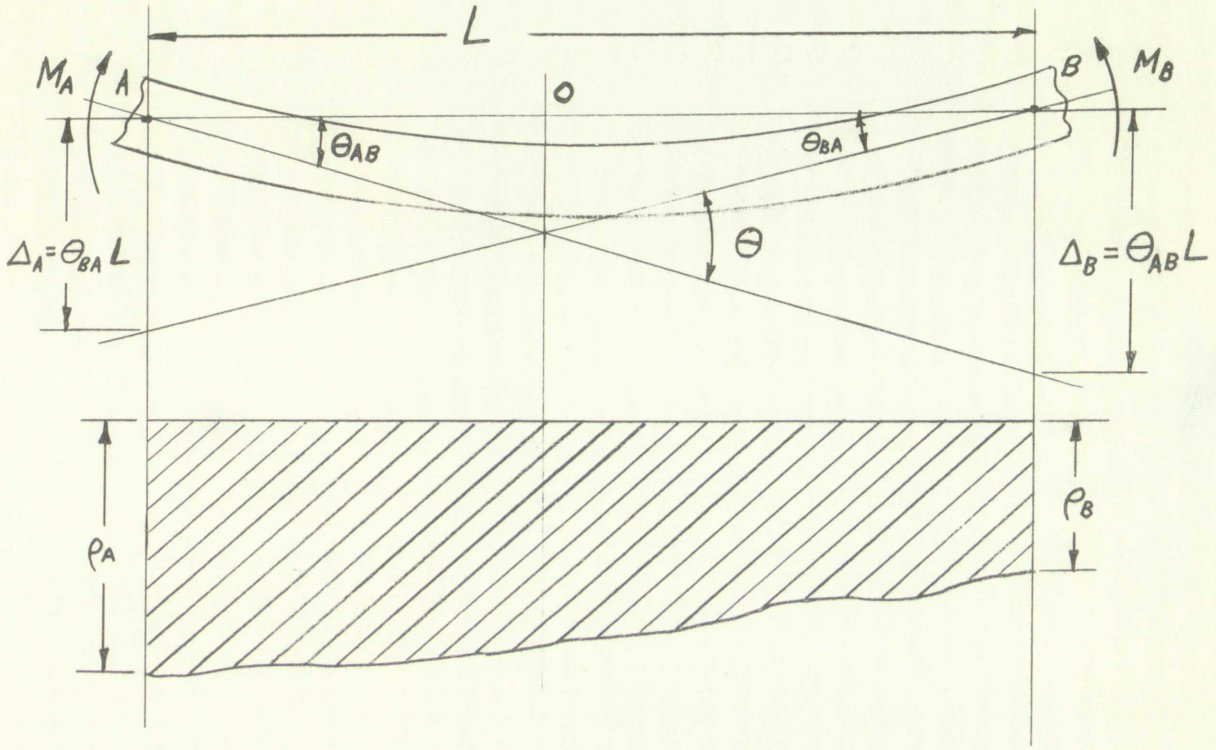

Figure 7

The second curvature-area theorem for deflection is also useful. It states: "The deflection of point B, from the tangent at point A, is equal to the static moment about an axis through B of the area under the curvature diagram between points A and B." Applying this to our example we write:

$$\Delta_A = \theta_{BA} \cdot L = \int_B^A \rho \cdot x \cdot dx$$

$$\Delta_B = \theta_{AB} \cdot L = \int_A^B \rho \cdot x \cdot dx \qquad (7)$$

This can be shown to be true by further consideration of Figure 7.

$$AO \cdot \theta_{AB} = BO \cdot \theta_{BA}$$

$$\theta = \theta_{AB} + \theta_{BA} = \text{Area under } \rho \text{ versus x diagram.}$$

Solving these two equations:

$$\theta_{AB} = \theta \frac{BO}{AB}$$

$$\theta_{BA} = \theta \frac{AO}{AB}$$

These values can be thought of in terms of a conjugate beam, the loading being the ρ versus x diagram. As previously shown, the area and therefore the total conjugate load is equal to θ. From the relationships between θ, θ_{AB}, and θ_{BA} the reactions are θ_{AB} and θ_{BA}. The dimensions

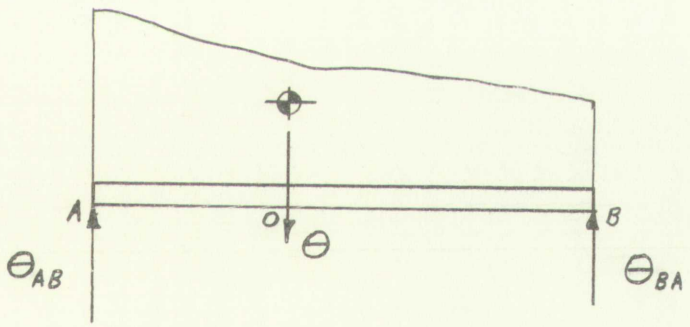

Figure 8

AO and BO describe the centroid of the area θ. Looking again at equation (7) we see that:

$$\theta_{BA} \cdot L = \theta \cdot AO = \text{moment of } \theta \text{ about A}$$

$$\theta_{AB} \cdot L = \theta \cdot BO = \text{moment of } \theta \text{ about B.}$$

This substantiates the second curvature-area theorem.

It is desirable to rewrite equation (7) in terms of curvature and moment. Looking at a free body of the member and realizing that Δ_A requires x to be measured from point A, we see:

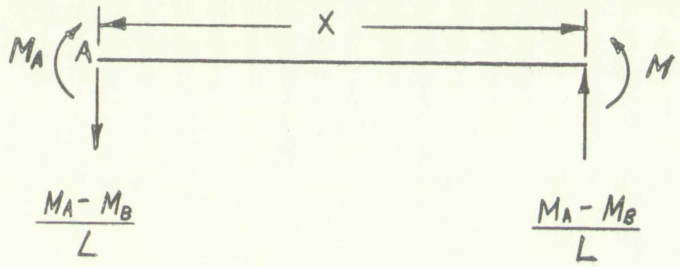

$$\Sigma M = 0$$

$$= M_A - [\ (\frac{M_A - M_B}{L})\ x\ ] - M = 0$$

$$M = M_A\ (1 - \frac{x}{L}\ ) + M_B\ \frac{x}{L}$$

$$x = \frac{M_A - M}{M_A - M_B} \cdot L$$

$$dx = - \frac{L}{M_A - M_B}\ dM$$

Rewriting equation (7) we have:

$$\Delta_A = \frac{L^2}{(M_A - M_B)^2}\ [\ \int_{M_A}^{M_B} \rho M\, dM - M_A \int_{M_A}^{M_B} \rho\, dM\ ] \qquad (8)$$

$$\theta_{BA} = \frac{L}{(M_A - M_B)^2} \left[\int_{M_A}^{M_B} \rho M \, dM - M_A \int_{M_A}^{M_B} \rho \, dM \right. \qquad (8a)$$

Equations (8) and (8a) are general expressions that are appropriate for both the elastic and plastic ranges. As proof of this condition we can substitute $\rho = \frac{M}{EI}$ into equation (8a) for the elastic range.

$$\theta_{BA} = \frac{L}{(M_A - M_B)^2 EI} \left[\int_{M_A}^{M_B} M^2 \, dM - M_A \int_{M_A}^{M_B} M \, dM \right]$$

$$= \frac{L}{(M_A - M_B)^2 EI} \left[\frac{M^3}{3} \Big|_{M_A}^{M_B} - M_A \cdot \frac{M^2}{2} \Big|_{M_A}^{M_B} \right]$$

$$= \frac{L}{6(M_A - M_B)^2 EI} \left[2M_B^3 - 2M_A^3 - 3M_A M_B^2 + 3M_A^3 \right]$$

$$= \frac{L}{6EI} \quad \frac{(M_A + 2M_B)(M_A^2 - 2M_A M_B + M_B^2)}{M_A^2 - 2M_A M_B + M_B^2}$$

$$= \frac{L}{6EI} (M_A + 2M_B) \qquad (8b)$$

Equation (8b) is recognizable as the slope-deflection expression for angular rotation in a member loaded only with end moments and unaffected by sidesway.

APPROXIMATION OF PLASTIC STRESS-STRAIN PROPERTIES

In reviewing approaches to simplification of stress-strain presentation, the two slope curve appears to be the most practical. As previously stated, this was the conclusion of Dwight. He pursued the matter and suggested a substitute curve. The data leading to such a recommendation was gathered from load versus deflection curves for British aluminum alloys D. T. D. 363A, HE15-WP, HE14-T, and NE7-M.

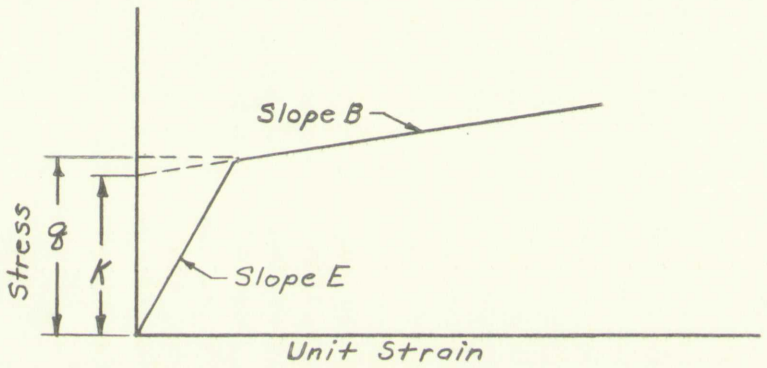

Figure 9

The shape of the curve is given in Figure 9.

Values of the various quantities are:

K - The average of stress values in tension and compression taken at a 0.1% offset ($\epsilon = 0.001$)

E - An average of Young's Moduli for the material in tension and compression

B - The average slope of tangents to the tension and compression curves drawn through a point on the stress axis equal to K

q - Stress at the intersection of the elastic and plastic curves.

For 6061-T6 the following values were found (see stress-strain curve Figure 1 in Appendix) :

$K = 39.4 \times 10^3$ lb./in.^{2}

$E = 10 \times 10^6$ lb./in.^{2}

$B = 14 \times 10^4$ lb./in.^{2}

Using equation (4) and a curve, as shown in Figure 9, for a rectangular beam, finite expressions for moment can be written. In this case, with the depth of section equal to h, c is equal to $\frac{h}{2}$ and:

$$\rho\frac{h}{2} < \frac{K}{E-B} \qquad M = \frac{Ebh^3}{12}\cdot\rho \tag{9a}$$

$$\rho\frac{h}{2} > \frac{K}{E-B} \qquad M = \frac{Kbh^2}{4} + \frac{Bbh^3\rho}{12} - \frac{K^3b}{3\rho^2(E-B)} \tag{9b}$$

(see Figure 2 of the appendix)

At this point it appears desirable to depart from a straight mathematical approach and associate deflections with material characteristics. For this purpose some new terms are introduced to assist in keeping the method general. First two letters representing integrals:

$$P = \int \rho\, dM \qquad Q = \int \rho M\, dM$$

These two integrals appear in equation (8). Next, three more non-dimensional quantities are offered as a means of using equation (9). They are:

$$m = \frac{M}{zK}$$

$$n = \frac{Eh\rho}{2K}$$

$$r = \frac{B}{E}$$

One unique value that represents the knee of the assumed stress-strain curve is given the symbol:

$$q = \frac{1}{1-r}$$ (see Figure 9)

Using all of the suggested ratios, equation (9b) can be rewritten:

$$\begin{aligned} n < q \qquad & m = n \\ n > q \qquad & m = \frac{3}{2} + rn - \frac{1}{2} \cdot \frac{q^2}{n^2} \end{aligned} \tag{10}$$

Since we are interested in deflections we must return to the consideration of quantities P and Q. We introduce two more dimensionless quantities:

$$\phi = \left(\frac{Eh}{2K}\right)\left(\frac{2}{M}\right) \int_o^M \rho \, dM = \left(\frac{Eh}{2K}\right)\left(\frac{2}{M}\right) P = \frac{2}{m} \int_o^m n \, dm$$

$$\delta = \left(\frac{Eh}{2K}\right)\left(\frac{3}{M^2}\right) \int_o^M \rho M \, dM = \left(\frac{Eh}{2K}\right)\left(\frac{3}{M^2}\right) Q = \frac{3}{m^2} \int_o^m n m \, dm$$

Using equation (10) in the expressions for ϕ and δ and performing the integration:

$$\begin{aligned} n < q \qquad & \phi = \delta = n = m \\ n > q \qquad & \phi = \frac{1}{m}\left[rn^2 + \frac{3}{1-r} - \frac{2}{n(1-r)^2} \right] \end{aligned} \tag{11}$$

$$\delta = \frac{1}{m^2}\left[r^2 n^3 + \frac{9}{4} rn^2 + \frac{5 - \frac{21}{4} r}{(1-r)^2} - \frac{9}{2} \cdot \frac{1}{1-r} \cdot \frac{q}{n} + \frac{1}{2} \cdot \frac{1}{1-r} \cdot \left(\frac{q}{n}\right)^3 - \frac{3}{2} \cdot \frac{r}{1-r^2} \cdot \log_e \frac{q}{n} \right] \tag{12}$$

From equations (10), (11), and (12) a family of curves can be drawn for materials with various values of E, B, and K.

With a complete representation of the material at hand, we can again return to the matter of structural analysis. Equation (8a) gives an expression for θ, a rotation caused by end moments. Extending this expression to include the terms in equations (10), (11), and (12) and adjusting the signs to accommodate clockwise moments (Figure 10), we have:

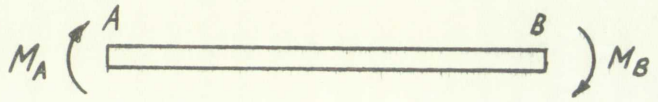

Figure 10

$$\theta_{AB} = \frac{L}{(M_A+M_B)^2} \left[M_B(P_A-P_B) + (Q_A+Q_B) \right]$$

$$\theta_{BA} = \frac{L}{(M_A+M_B)^2} \left[-M_A(P_A-P_B) + (Q_A+Q_B) \right] \qquad (13)$$

For a span of constant depth and without material variations, (13) can be further reduced remembering the values of P and Q:

$$\theta_{AB} = \frac{LK}{Eh(M_A+M_B)^2} \left[M_B(M_A\phi_A - M_B\phi_B) + \frac{2}{3}(M_A^2\delta_A + M_B^2\delta_B) \right]$$

$$\theta_{BA} = \frac{LK}{Eh(M_A+M_B)^2} \left[-M_A(M_A\phi_A - M_B\phi_B) + \frac{2}{3}(M_A^2\delta_A + M_B^2\delta_B) \right] \qquad (13a)$$

It should be noted that equation (8) was derived for the case of end moments only. The form of equations (8) through (13a) would not be changed by the inclusion of some lateral loading between the end points. Indeed such inclusions would be necessary if spans selected had lateral loads. Beyond the proportional limit superposition is not valid, as such, and the effect of loading could not be added to that of end moments.

Equation (13a) is exactly the same as the slope-deflection equations in that three unknowns, θ, M_A, and M_B, are related. Such equations could be written for each joint or sub-span of a structure. Solving all of the equations simultaneously would result in a complete description of moments and rotations at significant points. In practice the problem is complicated by the rather involved relationship of ϕ and δ to M. That is the reason for showing them (ϕ and δ) as separate quantities in equation (13a).

For structures that experience deflections commonly called sidesway, further alteration of equations (8) through (13a) would be necessary. Such considerations are not covered in this paper.

EXPERIMENTAL WORK

Within the confines of rather limited facilities and expenditures, an attempt was made to justify the use of equation (13a). While the apparatus had to be simple, it also had to embody enough resemblance to a practical problem to permit comparison. The selection was made of a portal frame with fixed ends. A square cross section was selected to simplify both the calculations and machining and to provide a member with high reserve strength. It also eliminated the problem of buckling and local crippling which are topics within themselves. The dimensions are shown in Figure 11.

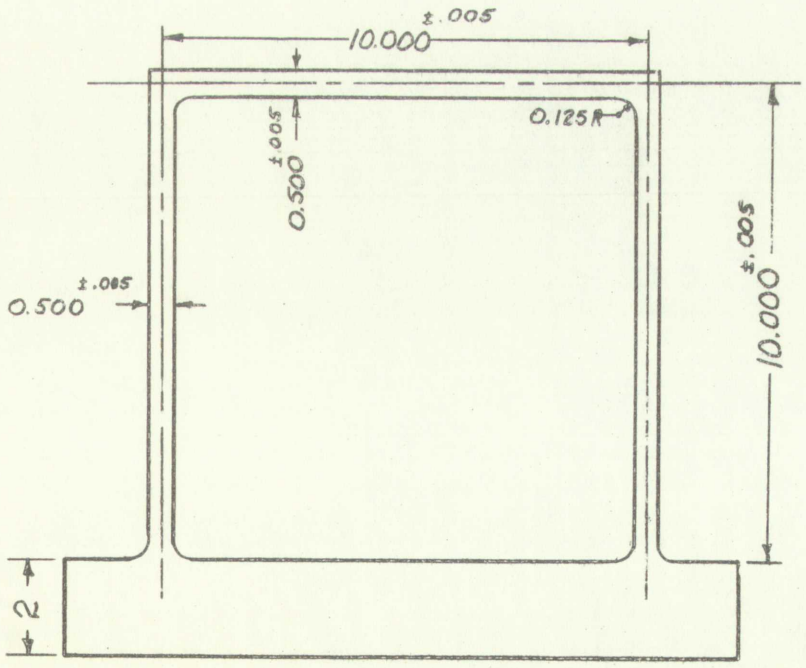

Figure 11

Material was 6061-T6 aluminum plate 0.500 inches thick, giving all members a 0.500 inch square cross section. The material orientation put the top span parallel to the longitudinal grain direction. All inside corners were given a radius of 0.125 inch to minimize stress concentration.

The point of load application was chosen as mid span as shown in Figure 12.

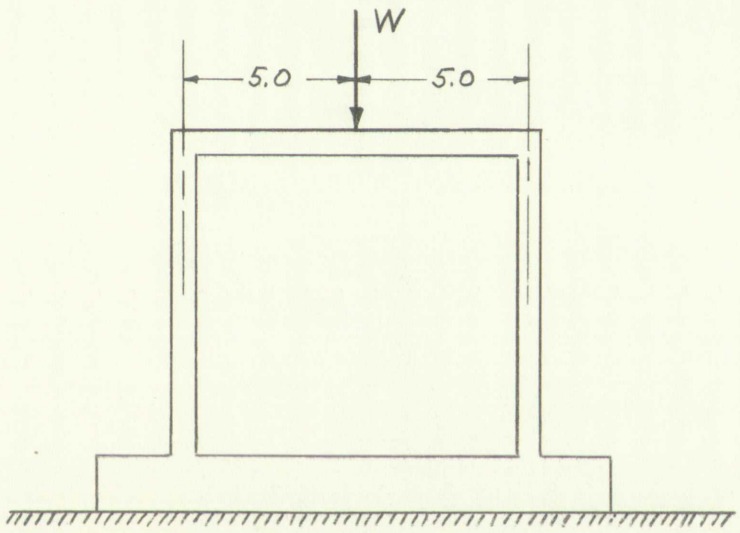

Figure 12

An elastic analysis for W = 100 lbs. produced the moments shown in Figure 13.

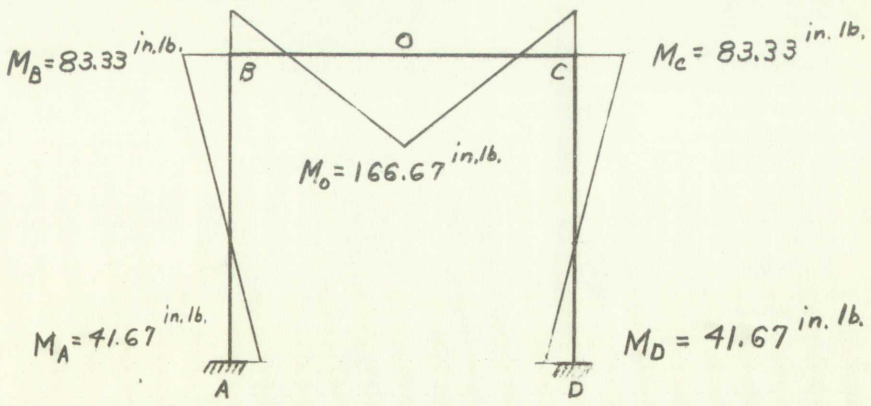

Figure 13

All testing was done on a Baldwin Tate-Emery Testing Machine, Type B. T. E., 120,000 lb. cap. using the 1,200 lb. and 6,000 lb. ranges and a load rate of approximately 20 lbs. per minute. The test set up is shown in Figure 8 of the Appendix. A dial indicator located directly under the load and supported at the top of the two columns gave deflections of point 0 versus points A and B. A plot of load versus deflections is given in Figure 3 of the Appendix. The actual deflection in the elastic range was slightly less than that predicted by conventional methods as shown in Table 1 of the Appendix.

In predicting the deflections beyond the proportional limit, equation (13a) was used. The steps were as follows:

1. Write equation for θ_{AB} and set equal to zero.

$$[\, M_B (M_A \phi_A - M_B \phi_B) + \frac{2}{3} (M_A^2 \delta_A + M_B^2 \delta_B) \,] = 0$$

2. Choose values of M_A and by trial and error satisfy the equation with values of M_B and from Figure 4 of the Appendix, ϕ_B and δ_B. This could be done by solving equations simultaneously, but it would be very difficult.

3. Knowing M_A and M_B solve for θ_{BA} using equation (13a). Table 2 of the Appendix.

4. By symmetry we know that point 0 has zero slope before and after loading. Therefore, the difference in slope between points B and 0 is equal to θ_{BA}.
   Subtracting θ_{OB} from θ_{BO} (or θ_{BA}) we have:

$$\theta_{BO} - \theta_{OB} = \theta = \frac{L}{M_O + M_B} (P_B - P_O)$$

   Knowing both θ and M_B, we solve for M_O again using Figure 4 of the Appendix. Table 3 of the Appendix.

5. Solve for θ_{OB}, the angle between a tangent to point 0 and a line through B and O. Table 4 of the Appendix.

   For small angles the deflection of point 0 is found by multiplying the angle θ_{OB} by the length OB. Table 4 of the Appendix.

The results of the predicted deflections are shown on the same plot as the actual results (Figure 3 of Appendix). As shown the predicted plastic values are larger than actually developed. This was also pointed out as being true in the elastic range. The discrepancy becomes more pronounced beyond the proportional limit. In the elastic range the elastic modulus and the exact cross sectional dimensions affect the results. Beyond this point these two values plus the assumed plastic modulus and the q or transition value also come in to play. These latter two have much the larger effect since they are arbitrary approximations. A re-run of the calculations for altered values of B and K could bring the two curves into line. Such altered values could then be used for any structural configuration of the same material. K, of course, denotes a form of yield point and can never be compared in percent deviation to something like a modulus which varies only slightly from one run to another and from one manufacturer to another. Part of the error resulting in the test work can be laid to the fact that the stress-strain curve, Figure 1 of the Appendix, was given as an average for the material.

The maximum load that the frame would accept was 1250 lbs. At this point, for all practical purposes, a plastic hinge was formed at points B, O, and C and deflection continued with no increase in load.

CONCLUSIONS

The actual deflections versus the predicted values showed a variation greater than the author had hoped. Reviewing the sources of error, however, shows that small corrections in assumed values could alter the picture. The encouraging aspect is that the actual and predicted curves took on very much the same shape. This would seem to indicate that the method is adaptable with further attention to exact material properties. In the final stages of deflection we see the actual values leveling off while the predicted values continue to rise. This is a quite obvious result of using B, the plastic modulus, equal to some value greater than zero. 6061-T6 in this regard turned out to be a poor choice for testing since its elongation before rupture is several times that of some other available alloys such as 2014-T6. This point could be argued two ways. But for the purpose of demonstrating that aluminum alloys resist the formation of collapse mechanisms common to mild steel, 6061-T6 was less co-operative.

None of the secondary affects such as buckling, crippling, axial load, etc. . . . was covered. The slenderness of the members coupled with a square cross section prevented their influencing the results to any predictable degree. These problems certainly exist, but they were considered beyond the scope of this paper.

Finally, it seems apparent that such a method with proper constants and improved technique can be a valuable tool in providing information on structural behavior beyond the elastic range.

APPENDIX

Table 1

LOAD Pounds	DEFLECTION - Inches Actual	Predicted
0	0	0
50	0.009	0.010
100	0.018	0.020
150	0.027	0.030
200	0.037	0.040
250	0.046	0.050
300	0.055	0.060
350	0.065	0.070
400	0.074	0.080
450	0.084	0.090
500	0.093	0.100
550	0.103	0.110
600	0.113	0.120
650	0.123	0.130
700	0.134	0.145
750	0.147	0.160
800	0.162	0.180
850	0.179	0.210
900	0.198	0.230
950	0.223	0.275
1,000	0.253	0.340
1,050	0.289	0.420
1,100	0.332	0.520
1,150	0.387	____
1,200	0.465	____

Table 2
Solving for θ_{BA}

① m_B	② M_B	③ ϕ_B	④ δ_B	⑤ $\frac{2}{3} M_B^2 \delta_B$ $\times 10^{-4}$	⑥ $M_B \phi_B$ $\times 10^{-4}$	⑦ M_A	⑧ $M_A^2(\frac{1}{3}\delta_A - \phi_A)$ $\times 10^{-4}$	⑨ $M_A M_B \phi_B$ $\times 10^{-4}$	⑩ $M_A + M_B$	⑪ $\frac{1}{(M_A+M_B)^2}$ $\times 10^{-7}$	⑫ ⑤+⑨−⑧ $\times 10^{-4}$	⑬ θ_{BA} = ⑪×⑫×6.0788
0.122	100	0.122	0.122	0.081	0.00122	50	0.0051	0.062	150	445.00	0.138	0.0048
0.244	200	0.244	0.244	0.650	0.00490	100	0.0410	0.490	300	111.10	1.100	0.0096
0.366	300	0.366	0.366	2.190	0.01095	150	0.137	1.640	450	49.40	3.690	0.0144
0.488	400	0.488	0.488	5.200	0.0195	200	0.324	3.900	600	27.80	8.780	0.0192
0.609	500	0.609	0.609	10.150	0.0304	250	0.635	7.600	750	17.80	17.100	0.0240
0.731	600	0.731	0.731	17.520	0.0426	300	1.110	12.700	900	12.35	29.100	0.0284
0.853	700	0.853	0.853	27.800	0.0596	350	1.740	20.800	1050	9.06	46.900	0.0336
1.000	821	1.000	1.000	45.000	0.0821	410	2.800	33.700	1231	6.59	75.900	0.0395
1.160	953	1.163	1.166	70.500	0.1083	477	4.410	44.400	1430	4.90	110.500	0.0427
1.257	1030	1.273	1.280	90.500	0.1312	515	5.550	67.600	1545	4.19	152.500	0.0504
1.346	1,104	1.392	1.411	114.500	0.1540	552	6.850	85,000	1656	3.65	192.600	0.0555
1.399	1,148	1.480	1.512	132.800	0.1700	574	7.690	97.500	1722	3.38	222.600	0.0594

Table 3
Solving for M_o

① $\theta_{oB} - \theta_{Bo} = \theta$	② $\theta \cdot \frac{Eh}{KL}$	③ M_B	④ ϕ_B	⑤ $M_B \phi_B$	⑥ M_o	⑦ ϕ_o	⑧ $M_o \phi_o$	⑨ $M_o\phi_o - M_B\phi_B$	⑩ $M_B + M_o$	⑪ $\frac{M_o\phi_o - M_B\phi_B}{M_B + M_o}$	⑫ $W = \frac{2}{5}(M_B + M_o)$	⑬ $\frac{M_B}{M_o}$
0.0192	0.488	400	0.488	195	800	0.975	780	585	1200	0.488	480	0.500
0.0240	0.610	500	0.609	304	995	1.223	1218	914	1495	0.610	598	0.503
0.0284	0.722	600	0.731	426	1,145	1.470	1,683	1,257	1745	0.720	698	0.524
0.0336	0.854	700	0.853	596	1,250	1.800	2,250	1654	1,950	0.850	780	0.566
0.0395	1.000	821	1.000	821	1,310	2.230	2,921	2,100	2,131	1.014	852	0.627
0.0427	1.085	950	1.163	1,105	1340	2.560	3430	2,480	2,290	1.080	916	0.709
0.0504	1.280	1,030	1.273	1,312	1,380	3.200	4416	3,104	2,410	1.288	964	0.746
0.0555	1.410	1,104	1.392	1,540	1,405	3.600	5,058	3,518	2,509	1.402	1,004	0.786
0.0594	1.510	1,148	1.480	1,700	1420	3.920	5,566	3,866	2,568	1.510	1,027	0.808

Table 4

Solving for θ_{oB} and Δ_o

①	②	③	④	⑤	⑥	⑦	⑧	⑨	⑩	⑪	⑫	⑬	⑭	⑮	⑯
M_B	ϕ_B	δ_B	$\phi_B - \frac{2}{3}\delta_B$	$\frac{M_B^2}{\times 10^{-4}}\left(\phi_B - \frac{2}{3}\delta_B\right)$	M_o	ϕ_o	δ_o	$\frac{M_B M_o \phi_o}{\times 10^{-4}}$	$\frac{2}{3} M_o^2 \delta_o \times 10^{-4}$	⑨+⑩-⑤ $\times 10^{-4}$	$M_B + M_o$	$\frac{(M_B + M_o)^2}{\times 10^{-4}}$	$\frac{LK}{Eh}\cdot\frac{1}{(M_B+M_o)^2}$ $\times 10^{8}$	θ_{oB} ⑪ × ⑭	Δ_o = 5.0 × ⑮
400	0.488	0.488	0.163	2,608	800	0.975	0.975	31.200	41.600	70,192	1200	144,000	2,736	0.019	0.095
500	0.609	0.609	0.203	5.075	995	1.223	1.226	60,900	80.885	136.710	1495	223,502	1.763	0.024	0.120
600	0.731	0.731	0.244	8.784	1,145	1.470	1.500	100,980	131.103	223.299	1745	304.503	1.294	0.029	0.145
700	0.853	0.853	0.284	13.916	1,250	1,800	1.922	157,500	200,156	343.740	1950	380,250	1.036	0.036	0.180
821	1.000	1.000	0.333	22.444	1,310	2,230	2.180	239,814	283,671	501.041	2,131	454.116	0.868	0.043	0.215
950	1.163	1.166	0.386	34.836	1,340	2.560	2.970	325,850	355.529	646.543	2290	524,410	0.751	0.049	0.245
1,030	1.273	1.280	0.420	44.558	1,380	3.200	3.820	459,848	485,051	895.341	2410	580,810	0.678	0.061	0.305
1,104	1.392	1.411	0.451	54.968	1405	3.600	4.380	558,103	576.415	1,079,850	2,509	629.508	0.626	0.068	0.340
1,148	1.480	1.512	0.472	62.205	1,420	3,920	4.770	638.977	641.215	1217.987	2,568	659.976	0.597	0.073	0.365

Figure 1

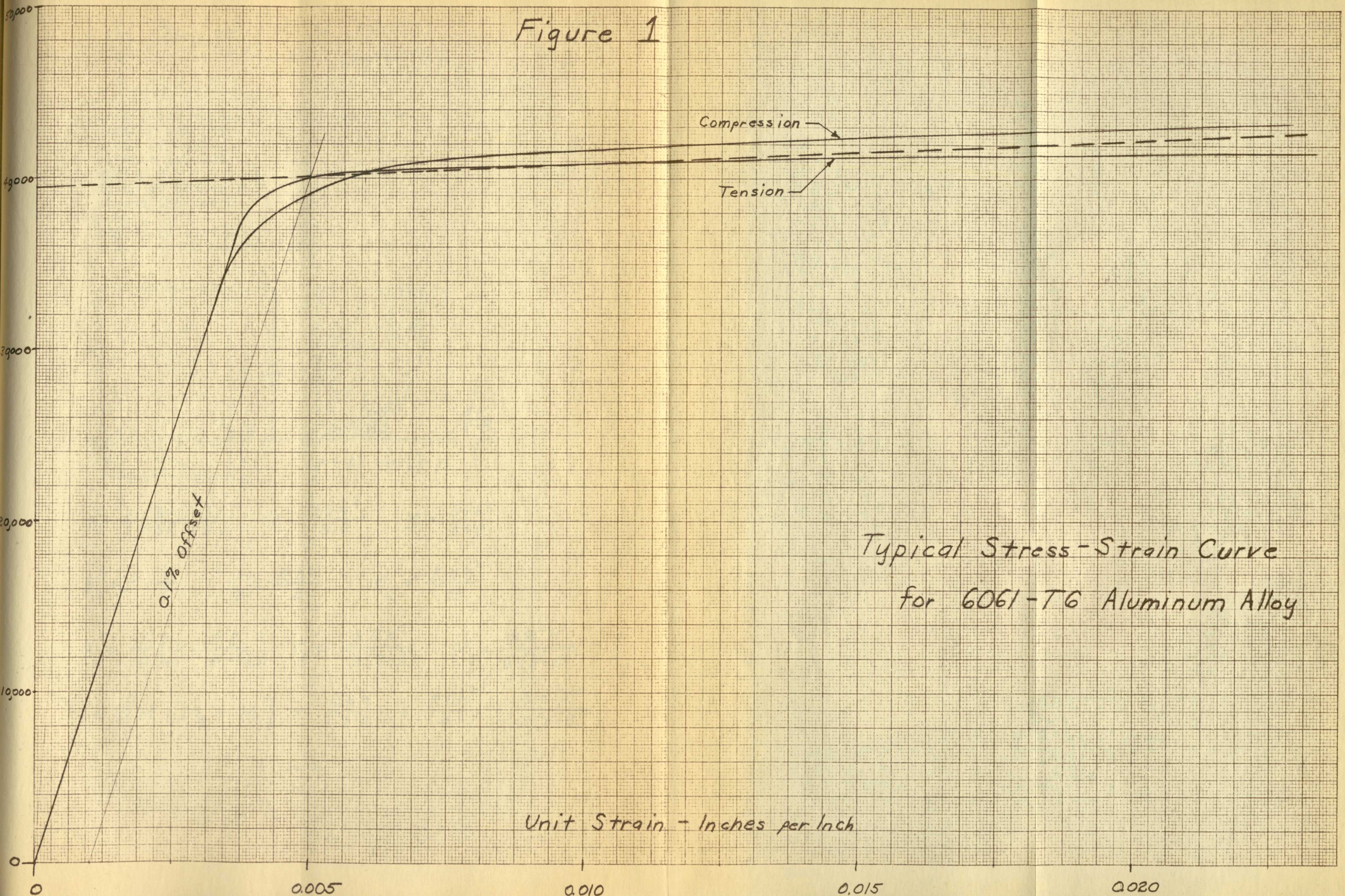

Typical Stress-Strain Curve
for 6061-T6 Aluminum Alloy

Development of Moment for Equation (9b)

A area under stress distribution curve
B plastic modulus
b width of member
E elastic modulus
f stress
h depth of member
K stress intercept
M moment
R radius of curvature
V volume under stress distribution curve

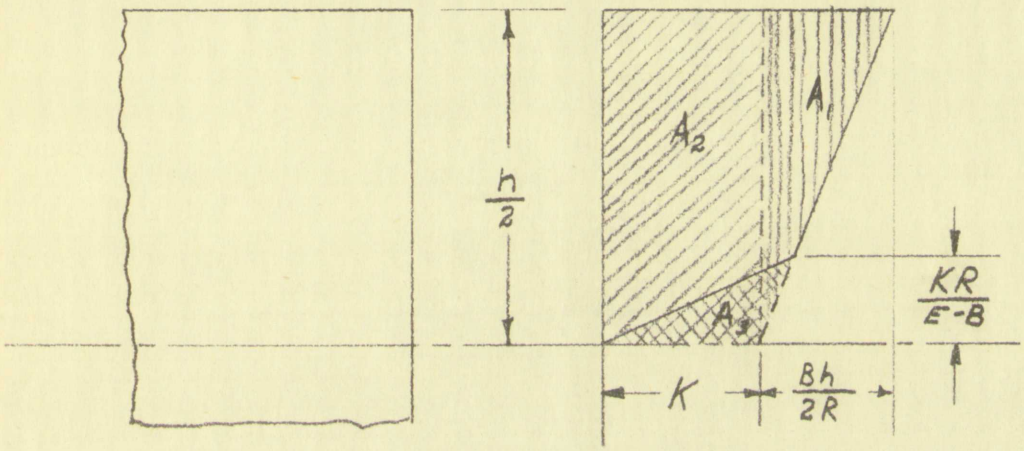

$$A_1 = \frac{1}{2}\left(\frac{Bh}{2R} \cdot \frac{h}{2}\right) \qquad V_1 = \frac{Bbh^2}{8R} \qquad M_1 = \frac{Bbh^3}{24R}$$

$$A_2 = K \cdot \frac{h}{2} \qquad V_2 = \frac{Kbh}{2} \qquad M_2 = \frac{Kbh^2}{8}$$

$$A_3 = \frac{1}{2}\left[K \cdot \frac{KR}{(E-B)}\right] \qquad V_3 = \frac{bRK^2}{2(E-B)} \qquad M_3 = \frac{bR^2K^3}{6(E-B)^2}$$

$$M = 2\left[M_1 + M_2 - M_3\right] = \frac{Bbh^3}{12R} + \frac{Kbh^2}{4} - \frac{bR^2K^3}{3(E-B)^2}$$

Figure 2

Figure 3

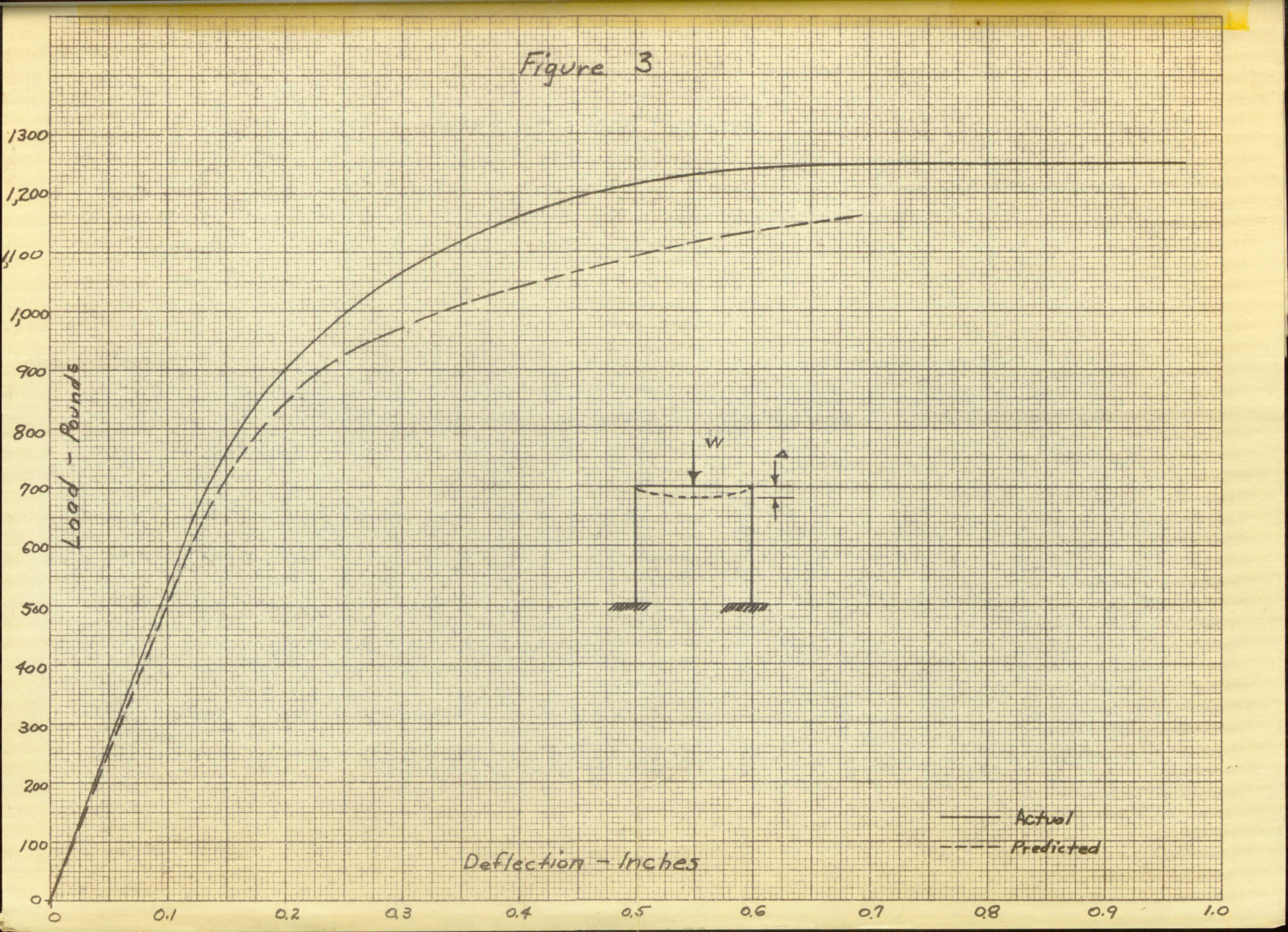
1300
1,200
1,100
1,000
900
800
700
600
500
400
300
200
100
0
Load - Pounds
0
0.1
0.2
0.3
0.4
0.5
0.6
0.7
0.8
0.9
1.0
Deflection - Inches
W
Actual
Predicted

Figure 4

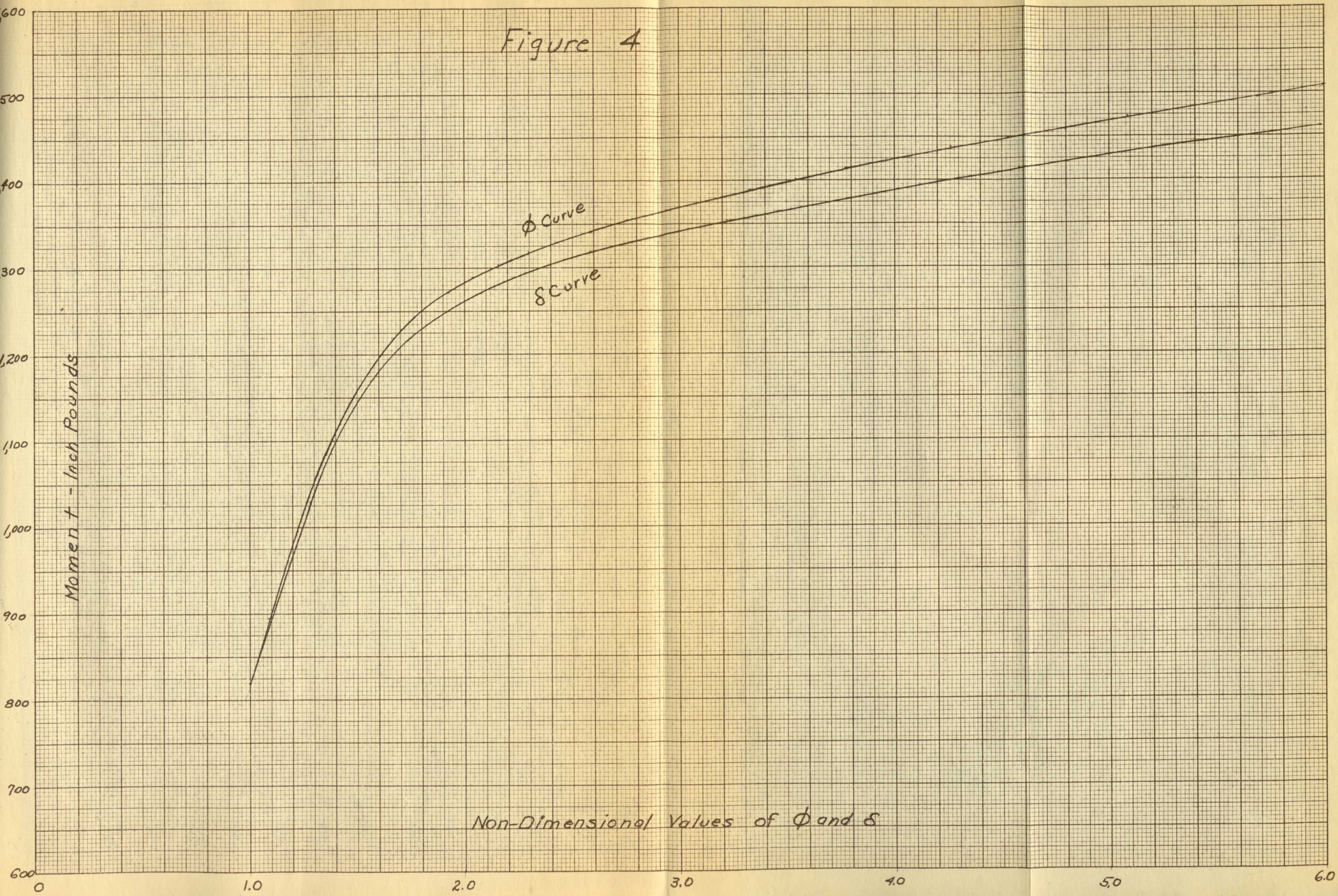
600
500
400
300
1,200
1,100
1,000
900
800
700
600
Moment - Inch Pounds
φ Curve
δ Curve
Non-Dimensional Values of φ and δ
0
1.0
2.0
3.0
4.0
5.0
6.0

Figure 5

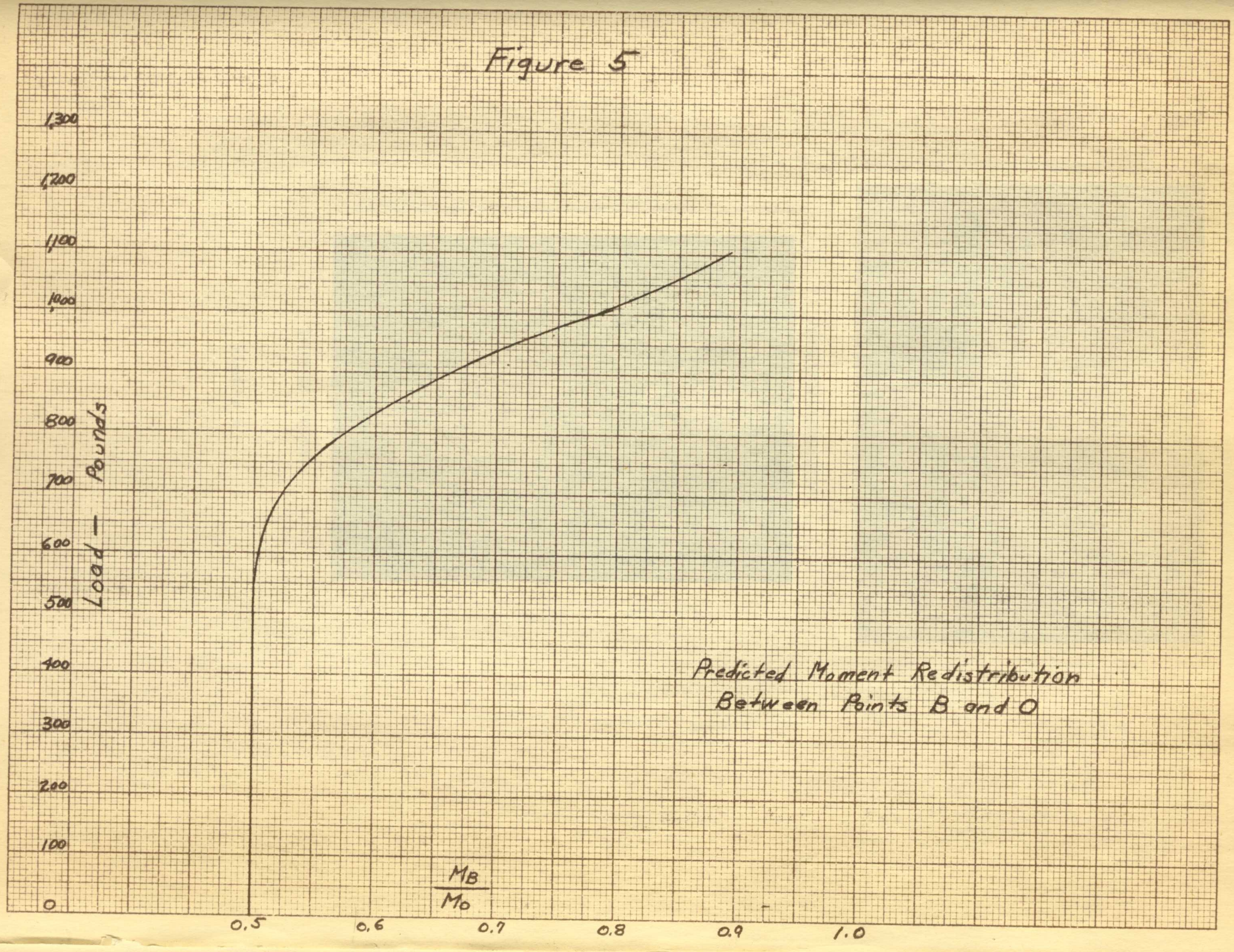
1,300
1,200
1,100
1,000
900
800
700
600
500
400
300
200
100
0
Load — Pounds
0.5
0.6
0.7
0.8
0.9
1.0
MB / MO
Predicted Moment Redistribution
Between Points B and O

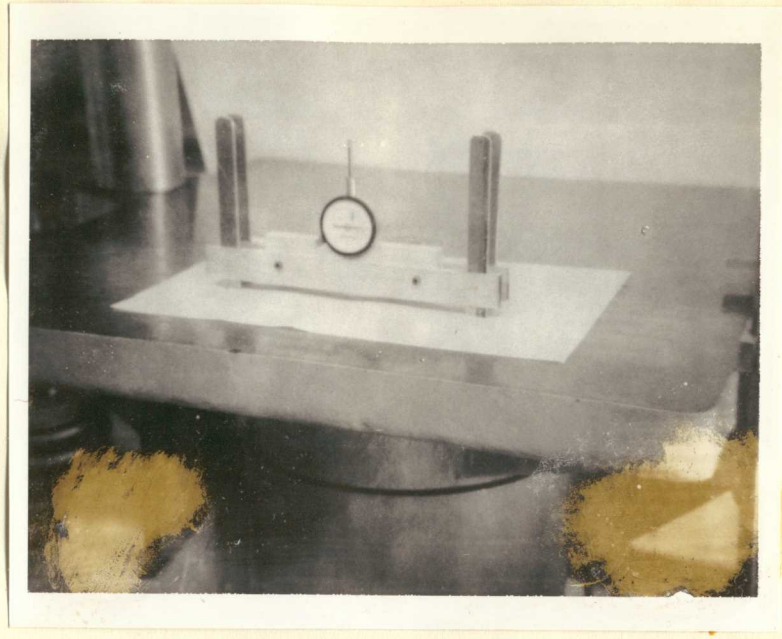

Indicator Support

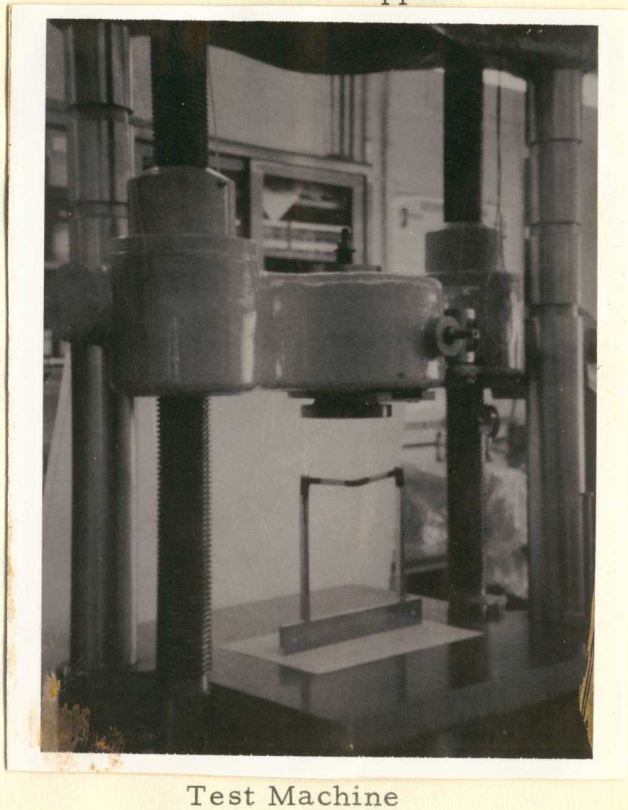

Test Machine

Figure 6

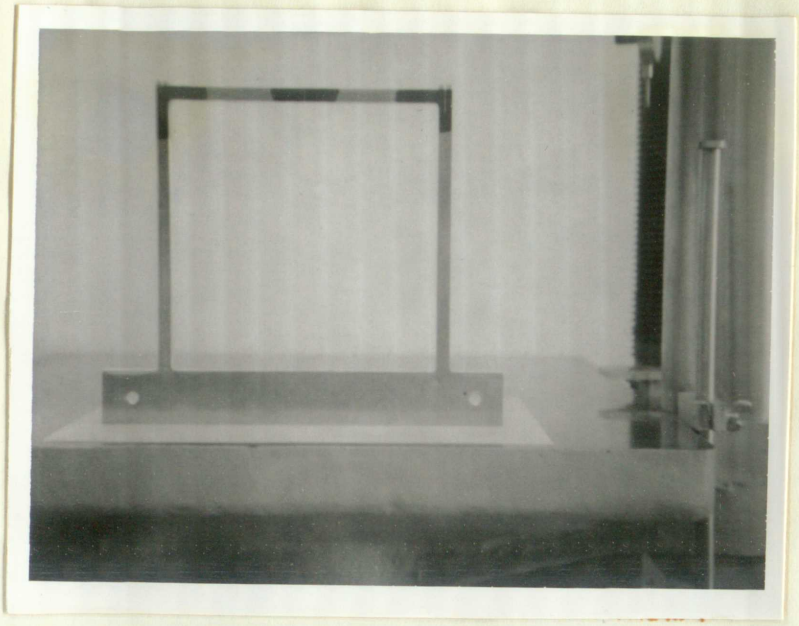

Before Loading

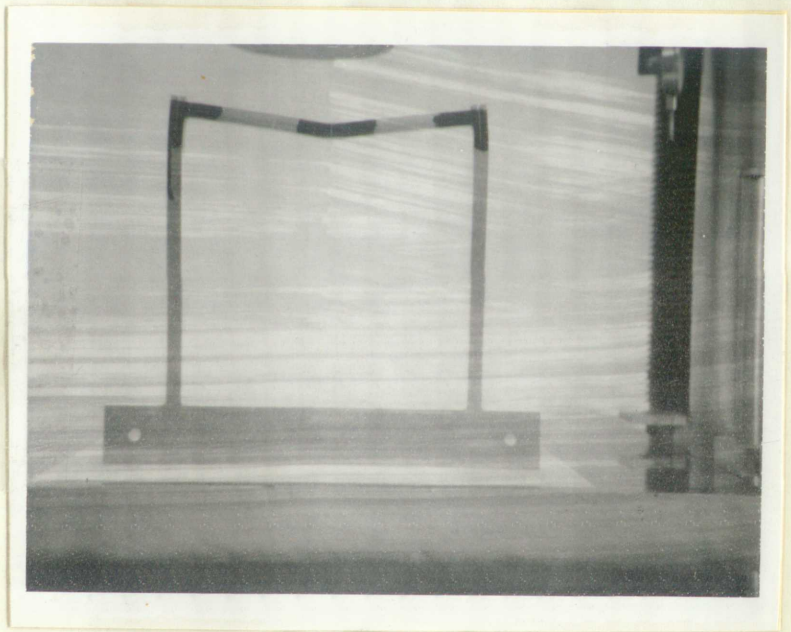

After Loading

Figure 7 Test Frame

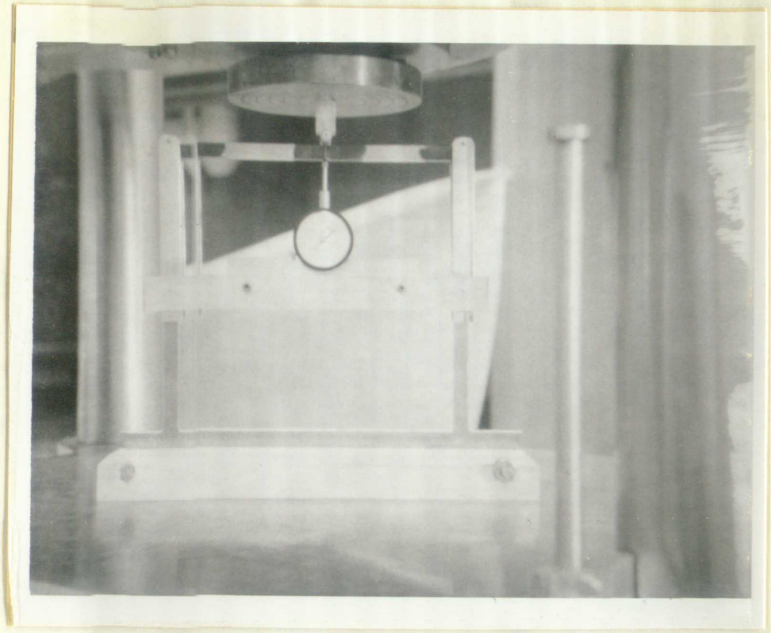

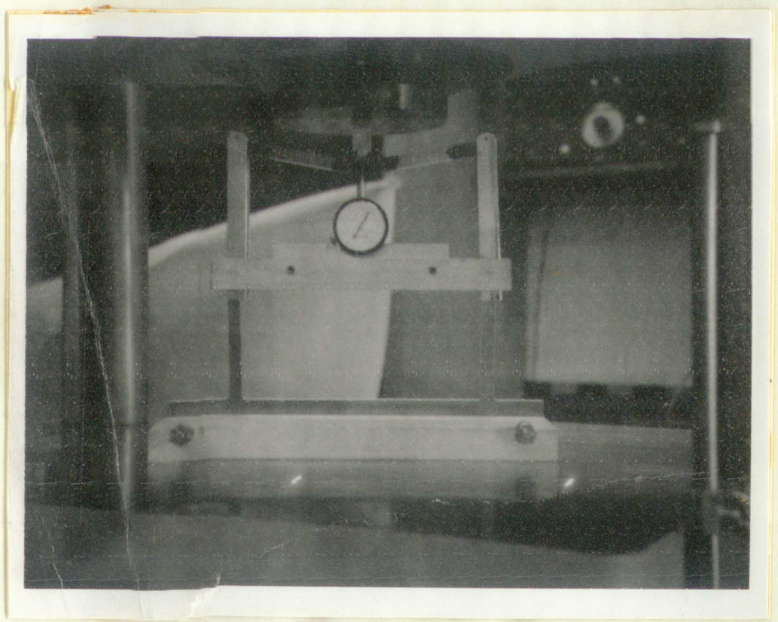

Figure 8 Loading Sequence

REFERENCES

1. Alcoa Structurall Handbook, Aluminum Company of America, Ptt.., 1958.

2. Strength of Metal Aircraft Elements, Mil-HDBK-5 March 1959.

3. Plastic Design iin Steel, American Institute of Steel Construction, Inc.,, New York, May 1959.

4. Timoshenko, S.. Strength of Materials, Part II, D. van Nostrand, New York, 1946.

5. Panlilio, F. "The Theory of Limit Design Applied to Magnesium Alloyy and Aluminum Alloy Extrusions," Journal Royal Aero. Soc., Jan. 1947.

6. Cozzone, F. P.. "Bending Strength in the Plastic Range," Journal Aero. Sci., May 1943.

7. Wang, T. K. "Elastic and Plastic Bending of Beams," Journal Aero. Sci., July 1947.

8. Osgood, W. E. "Stress and Strain Formulas," Journal Aero. Sci., Jan. 1946.

9. Beilschmidt, J. L. "The Stress Developed in Sections Subjected to Bending Moment," Journal Aero. Sci., July 1942.

10. Gill, S. S. "Bending Strength of Materials with a Non-linear Stress-Strain Curve," Aircraft Engineering, July 1947.

11. Dwight, J. B. "An Investigation into the Plastic Bending of Aluminum Alloy Beams," The Aluminum Development Association Report No. 16, The Kynoch Press, Birmingham, England, 1953.